Leaflet No- 13/2020

The Republic of the Union of Myanmar
Ministry of Natural Resources and Environmental Conservation
Forest Department

Assessment of natural recovery of mangrove from anthropogenic disturbance using neural network-based classification of satellite images

Win Sithu Maung, Staff Officer
Forest Department

Table of Contents

Assessment of natural recovery of mangrove from anthropogenic disturbance using neural network-based classification of satellite images

Win Sithu Maung, Staff Officer

Forest Department

Abstract

Since mangrove forests around the world are declining due to human disturbances such as shrimp farming, agricultural expansion, urbanization, and over-harvesting for fuelwood, rehabilitation programs should be accelerated for mangrove conservation urgently. Many studies pointed out that the current popular artificial planting approach yielded an unsatisfactory surviving rate for extensive plantations due to the lack of a site-species match. Limited studies focused on natural recovery of mangrove that is an opportunity for mangrove rehabilitation. Hence, the present study examined natural recovery mangrove from different abandoned shrimp ponds through spatial and species analysis. Before any restoration programs, knowing the actual distribution of regional mangrove extent is of great importance for implementation of mangrove rehabilitation and formulation of necessary regulations. Due to the inaccessibility of mangrove nature, remote sensing classification is a time and cost-effective approach to obtain reliable information of extensive mangrove forests. Although a number of studies have applied different classification methods combining with various remotely sensed data for mangrove distribution, there is lack of information about the performance of artificial neural network (ANN) using Sentinel-2 imagery for mangrove classification. In this dissertation, artificial neural network was therefore employed with the combination of Sentinel-2 satellite images in order to propose a promising classification approach for a large extent of mangrove areas. This study firstly conducted two main experiments of input features and hyper-parameter tuning since input features play a key role to improve resultant accuracy in remote sensing classification as has a selection of method deployed. Through these two main experiments, mangrove distribution of the study area, Wunbaik Mangrove Forest (WMF) in 2020 could be classified with overall accuracy of 95.98% and kappa coefficient of 0.92. Transfer learning improved the performance of the model in classifying a new dataset in 2015 and the resultant overall accuracy and kappa coefficient were 97.20% and 0.94. Secondly, the study fulfilled information about mangrove changes in WMF from 2015 and 2020 through post-classification change detection. The result of change detection showed that mangrove areas in WMF slightly declined between 2015 and 2020 because of shrimp pond expansion for local livelihoods. Lastly, natural recovering mangrove areas from shrimp farming activities were delineated in terms of spatial and species analysis integrating field survey data. As a result, the study found that mangrove forests can naturally recover around 50 % of a shrimp pond without any restoration effort during a short period of abandonment. Furthermore, recovering mangrove species are diversely distributed at different abandoned ponds depending on their environmental preference. *Avicennia officinalis* and *Avicennia marina* are dominant species with high adaptability to different salinity and elevation range in the early mangrove community recovering at abandoned shrimp ponds. According to research findings, this study reveals that artificial neural network classification using Sentinel-2 image produces a promising accuracy for mangrove distribution and integration of digital terrain and canopy height models can improve resultant accuracy in mangrove classification. Protection measures for existing mangrove should be more enhanced to prevent conversion to other land uses while natural recovery of mangrove is supporting mangrove rehabilitation effectively.

Keywords: mangrove; natural recovery; artificial neural network; Sentinel-2; transfer learning; change detection

Neural Network အခြေပြု Satellite Image Classification နည်းလမ်းဖြင့် လူသားတို့၏ဖျက်ဆီးမှုများမှ ဒီရေတောများ သဘာဝအတိုင်းပြန်လည်ဖြစ်ထွန်းလာမှုကို လေ့လာဆန်းစစ်ခြင်း

စာတမ်းအကျဉ်း

ကမ္ဘာအဝှမ်းရှိ ဒီရေတောများသည် ပုစွန်မွေးမြူခြင်း၊စိုက်ပျိုးမြေချဲ့ထွင်ခြင်း၊ မြို့ပြတိုးချဲ့ခြင်းနှင့် ထင်းလောင်စာအလွန်အကျွံထုတ်ယူခြင်းစသည့် လူသားတို့၏ နှောက်ယှက်ဖျက်ဆီးမှုများ ကြောင့် ပျက်စီးပြုန်းတီးလျက်ရှိနေသဖြင့် ဒီရေတောပြန်လည်ဖြစ်ထွန်းရေး လုပ်ငန်းအစီစဉ်များ အရေးတကြီး ချမှတ်ရန် လိုအပ်လျက်ရှိပါသည်။ သုတေသနတွေ့ရှိ ချက်များအရ ကေအများ အပြား စိုက်ပျိုးကြသည့် ဒီရေတော စိုက်ခင်းကြီးများတွင် စိုက်ပျိုးမည့်နေရာနှင့် ရွေးချယ်သည့် သစ်မျိုး မကိုက်ညီမှုများကြောင့် စိုက်ခင်းရှင်သန် အောင်မြင်မှု နည်းပါးတတ်သည်ကို တွေ့ရှိရပါသည်။ သို့သော်လည်း ဒီရေတောများ ပြန်လည်ဖြစ်ထွန်းရေးအတွက် အခွင့်အလမ်းကောင်း တစ်ခုဖြစ်သော သဘာဝအတိုင်း ဒီရေတောများ ပြန်လည်ဖြစ်ထွန်း လာမှုကို သုတေသနလေ့လာ ပြုစုမှုနည်းပါးနေပါသည်။ သို့ဖြစ်ပါ၍ ယခုလေ့လာမှု သည် ရခိုင်ပြည်နယ် ဝန်ဗိုက်ဒီရေတောရှိ စွန့်ပစ်ပုစွန်ကန် အမျိုးမျိုးတွင် ဒီရေတောများ သဘာဝအတိုင်းဖြစ်ပေါ်လာမှုကို ဧရိယာနှင့် သစ်မျိုုးဆန်းစစ် ချက်မှ ပြုလုပ်ထားသည့် သုတေသနတစ်ခုဖြစ်ပါသည်။ ဒေသအတွင်း လက်ရှိ ဒီရေတော ပမာဏကို သိရှိခြင်းသည် ဒီရေတော ပြန်လည် ဖြစ်ထွန်းရေး လုပ်ငန်းများ အကောင်အထည် ဖော်ခြင်းနှင့်လိုအပ်သည့် မူဝါဒများ ချမှတ် နိုင်ရေးတို့အတွက် ဒီရေတောပြုစု ပျိုးထောင်ရေး လုပ်ငန်းများမစမီ အရေးတကြီး သိထားရမည့် အချက် တစ်ခုဖြစ်ပါသည်။ ဒီရေတော ဧရိယာများတွင် သွားလာအုပ်ချုပ်ရန် ခက်ခဲမှုတို့ကြောင့် အဝေးမှစူးစမ်း လေ့လာခြင်း (Remote Sensing) နည်းပညာ သည် ကျယ်ပြန့်သည့် ဒီရေတောဧရိယာများအတွက် ယုံကြည်စိတ်ချရသော သတင်းအချက် အလက်များပေးစွမ်းနိုင်သည့် အချိန်နှင့်ငွေကြေး ကုန်ကျမှုများ သက်သာသော နည်းပညာ တစ်ခုဖြစ်ပါသည်။ ဒီရေတောဧရိယာ များခွဲခြားဖော်ထုတ်ခြင်း (Mangrove Classification) နည်းလမ်းများစွာကို အမျိုးမျိုးသော Satellite Images များအသုံးပြု၍ လေ့လာပြီး ဖြစ်ကြသော်လည်း Artificial Neural Network (ANN) နည်းလမ်းနှင့် Sentinel-2 Satellite Images တို့ကို အသုံးပြု၍ လေ့လာထားသည့် သုတေသနများမရှိသေးကြောင်း တွေ့ရှိရ ပါသည်။ ယခုသုတေသနတွင် Mangrove classification အတွက် အသုံးပြုသည့် အချက်အလက်များ ပေါင်းစပ်အသုံးပြုမှု (Input Feature Combination) နှင့် ANN model အတွင်း hyper-parameters များ ချိန်ညှိစမ်းသပ်မှုများကို စတင်ပြုလုပ်ခဲ့ပါသည်။ ထိုစမ်းသပ်မှု (၂)မျိုးမှ ရရှိလာသော ANN model ကို အသုံးပြု၍ ၂၀၂၀ ခုနှစ်ရှိ ဒီရေတောများကို ခန့်မှန်းရာတွင်

Overall Accuracy ၉၅.၉၈% နှင့် Kappa အညွှန်းကိန်း ၀.၉၂ ရရှိခဲ့ပါသည်။ ၎င်း ANN model ကို Transfer Learning နည်းလမ်းဖြင့် တိုးတက်အောင်ပြုလုပ်ပြီး ၂၀၁၅ ခုနှစ်ရှိ ဒီရေတော ပြန့်နှံ့ပေါက်ရောက်မှုများကို ခန့်မှန်းခဲ့ရာ Overall Accuracy ၉၇.၀၀% နှင့် Kappa အညွှန်း ကိန်း ၀.၉၄ ရရှိခဲ့ပါသည်။ ထိုနောက် ၂၀၁၅ ခုနှစ်နှင့် ၂၀၂၀ခုနှစ်အတွင်း ဒီရေတော ပြောင်းလဲမှုများကို Post classification Change detection နည်းလမ်းဖြင့် လေ့လာခဲ့ရာ ရခိုင်ပြည်နယ်ရှိ ဝန်ဗိုက်ဒီရေတောအတွင်း ပုစွန်ကန်တိုးချဲ့မှုများကြောင့် ဒီရေတောဧရိယာ အနည်းငယ် လျော့နည်းသွားသည်ကို တွေ့ရှိခဲ့ရပါသည်။ ကွင်းဆင်းကောက်ယူ ခဲ့သော အချက် အလက် များအား Post classification Change detection နည်းလမ်းမှရရှိသော ရလဒ် များနှင့်ပူးပေါင်းကာ ဒီရေတောများသဘာဝ အတိုင်းဖြစ်ပေါ်လာမှုကို ဧရိယာနှင့် သစ်မျိုး ဆန်းစစ်မှုပြုလုပ်ခဲ့ရာတွင် ဒီရေတောများသည် စွန့်ပစ်ပုစွန်ကန်တစ်ခုတွင် မည်သည့် ပြန်လည်ပြုစု ပျိုးထောင်ခြင်းလုပ်ငန်းများမှ ဆောင်ရွက်ရန် မလိုဘဲ အချိန်ကာလ တိုအတွင်း ဧရိယာ၏ ၅၀% ထိ သဘာဝအတိုင်းပြန်လည် ဝင်ရောက် လာနိုင်ကြောင်း တွေ့ရှိခဲ့ရပါသည်။ သဘာဝအတိုင်းပြန်လည် ဝင်ရောက်လာသည့် ဒီရေတော သစ်မျိုးများသည် ၎င်းတို့ နှစ်သက်သည့် ပတ်ဝန်းကျင်အချက်လက်များ (Water Salinity နှင့် Elevation) ပေါ်မူတည်ပြီး ပြန့်နှံ့ပေါက်ရောက် နေကြောင်းကိုလည်း တွေ့ရှိခဲ့ရပါသည်။ *Avicennia officinalis* (သမဲကြီး)နှင့် *Avicennia marina* (သမဲ့ဖြူ) တို့သည် အမျိုးမျိုးသော Water Salinity နှင့် Elevation တို့တွင် ရှင်သန်ပေါက်ရောက်နိုင်သည့် အများဆုံးတွေ့ရသော သစ်မျိုးများဖြစ်ပါ သည်။ ယခုသုတေသနတွေ့ရှိချက်များအရ Sentinel-2 Satellite image ကို အသုံးပြုသော ANN နည်းလမ်းသည် ဒီရေတောများပြန့်နှံ့မှုကိုသိရှိရန် အတွက် တိကျခိုင်မာသည့် ရလဒ်ကောင်းများပေးစွမ်းနိုင်သော နည်းလမ်းတစ်ခုဖြစ်ကြောင်း ဖော်ထုတ်နိုင်ခဲ့ပါ သည်။ ထို့အပြင် ဒီရေတော ရွက်အုပ်အမြင့် နှင့် မြေမျက်နှာသွင်ပြင် အမြင့်တို့ ထည့်သွင်းအသုံးပြု ခြင်းဖြင့် Mangrove classification တွင် Overall Accuracy ကို တိုးမြှင့်ရရှိနိုင်ပါသည်။ သို့ဖြစ်ပါ၍ ဒီရေတောများ ပြန်လည်ဖြစ်ထွန်းလာစေရေးအတွက် သဘာဝအတိုင်း ပြန်လည် ဖြစ်ထွန်း လာမှု (Natural Recovery) သည် ထိရောက်စွာ ထောက်ပံ့ပေးနေစဉ်တွင် လက်ရှိ ကျန်ရှိနေသေးသော ဒီရေတောဧရိယာများမှ အခြားမြေ အသုံးချမှုများသို့ ပြောင်းလဲမသွား စေရန် ထိန်းသိမ်းရေးလုပ်ငန်းစဉ် များအား အရှိန်အဟုန် မြှင့်ဆောင်ရွက်သင့်ပါသည်။

Assessment of Natural Recovery of Mangrove from Anthropogenic Disturbance using Neural Network-based Classification of Satellite Images

1. Introduction

Mangroves are a salt-tolerant forest community which occurs especially in tropical and subtropical intertidal portions of the world[1]. They provide magnificent ecosystem services that are not only tangible goods such as wood and non-wood products but also intangible services such as protecting coastal regions from storm and wave, and acquisition of massive amounts of carbon dioxide[2]. Despite such invaluable ecosystem services, mangrove forests around the world were being depleted with an alarming rate year by year due to human pressures such as the development of aquaculture, agricultural expansion, oil plantations, and urbanization[3]. In order to compensate for mangrove loss, restoration projects have been implemented primarily by means of artificial plantations. Many studies pointed out that plantation projects may lead to unsatisfied results with low survival rates when a replanted mono-species is not appropriate for a selected site. One of the opportunities is that mangrove possesses a high capacity of self-recovery in which mangrove species can naturally reenter a deforested area if environmental parameters such as natural hydrology, salinity, and elevation of a site meet the preferences of seeds or propagules dispersed along with tidal flow. However, little attention has been paid to the natural recovery of mangrove in considering rehabilitation programs.

The study area of this research, Wunbaik Mangrove Forest (WMF), plays a vital role in providing ecological, environmental, and socio-economic goods and services to the local community. However, due to aquaculture and agricultural expansions, WMF and its surrounding mangrove forest have been highly degraded since the 1990s. According to FAO inventory in 2011 [4], WMF possesses a high capacity of recovery due to abundant seed productivity and high germination rate of mangrove species. Therefore, this region is suitable to explore natural recovery of mangrove from human disturbances. Despite such a large remnant mangrove extent, there is a prominent gap of information about mangrove distribution and changes after 2014. For sustainable mangrove management, updated and accurate information is necessary before implementing any restoration efforts.

Being that mangroves are not only under natural and anthropogenic threats but also growing in remote areas, accessibility of reliable and accurate information is difficult for a large extent of mangrove[5]. With the development of technology in the remote sensing field, advanced approaches were improved to satellite image classification in various disciplines. Remote sensing plays an important role in monitoring mangrove distribution and identifying species, and other attributes such as estimating tree height and biomass. Developing space technology and agencies, satellite data for mangrove areas around the world are accessible and helpful to overcome management barriers in the mangrove field. Still, the interpretation of the remotely sensed data into usable information is challenging due to the complexity of the targeted field. Therefore, features acquired by the earth sensors are needed to perform a further analysis in order to translate into more reliable and understandable information.

Classification is one of the important approaches, which can offer promising information of earth objects by analyzing remotely sensed data from satellite sensors. However, classification accuracy varies depending on not only usage of remotely sensed data but also choice of appropriate classifier[6]. For mangrove distribution, several classification approaches have been developed and explored by using different classifiers and satellite imageries. In recent advanced classification methodologies, machine learning is a new emerging field and classifiers such as artificial neural network (ANN), random forest (RF) and support vector machine (SVM). Among these different methods, ANN has become more popular and widely used in many fields by combining remotely sensed satellite images because of producing a promising result and robustness of the model [7]–[10].

Launching Sentinel-2 satellite by European Space Agency in 2015 was a great opportunity for the remote sensing community to develop classification approaches for a different variety of fields[11]. With the advantages of spectral, temporal, and spatial resolutions of freely accessible multispectral bands, Sentinel-2 imagery outperformed Landsat 8 by yielding more precise results in remote sensing classification[12]–[14]. Also, in mapping of mangrove extent and species, Wang et al [15] described that Sentinel-2 sensor bested Landsat 8 by offering more accurate information in their research.

Applying such benefits of ANN method and Sentinel-2 imagery, some studies could improve the results in their targeted fields [16]–[20]. Although there are limited studies of mangrove using ANN classification with different satellite images, due to the outperformance of recently launched Sentinel-2 imagery, it is worth investigating potential performance of artificial neural network classification in collaboration with Sentinel-2 imagery for mangrove distribution. Through this proposed approach, a promising result for mangrove classification would be achieved in order to provide the lack of information about mangrove changes in the WMF and assess natural recovery of mangrove after human disturbances.

2. Objectives

Basically, the study has three folds; (a) artificial neural network classification, (b) change detection, and (c) natural recovery process of mangrove after human disturbances. The main objectives are mentioned as follows;

i. To explore artificial neural network classification in collaboration with Sentinel-2 imagery for mangrove distribution,
ii. To fulfill information gap of mangrove changes in the WMF between 2015 and 2020 through post classification change detection, and
iii. To assess natural recovery process of mangrove after human disturbances by comparing different abandoned shrimp ponds in terms of spatial and species analysis

3. Materials and Methods

3.1. Study site

The study area was located between 19°07'0"–19°23'30"N and 93°51'0"– 94°02'30"E in Yambye Township, Kyauk Phyu District, Rakhine State, Myanmar (Figure 1). Mangrove forests in the study area are locally known as the WMF, of which the main portion of mangroves are part of a reserved forest known as the Wunbaik Reserved Mangrove Forest (WRMF), formally protected by the Forest Department since 1931. WRMF is one of the largest remaining mangrove communities, with an area of 22919 ha[4][21]. The FAO has identified 34 mangrove species such as *Rhizophora, Avicennia, Sonneratia* in WRMF since 2011[22].

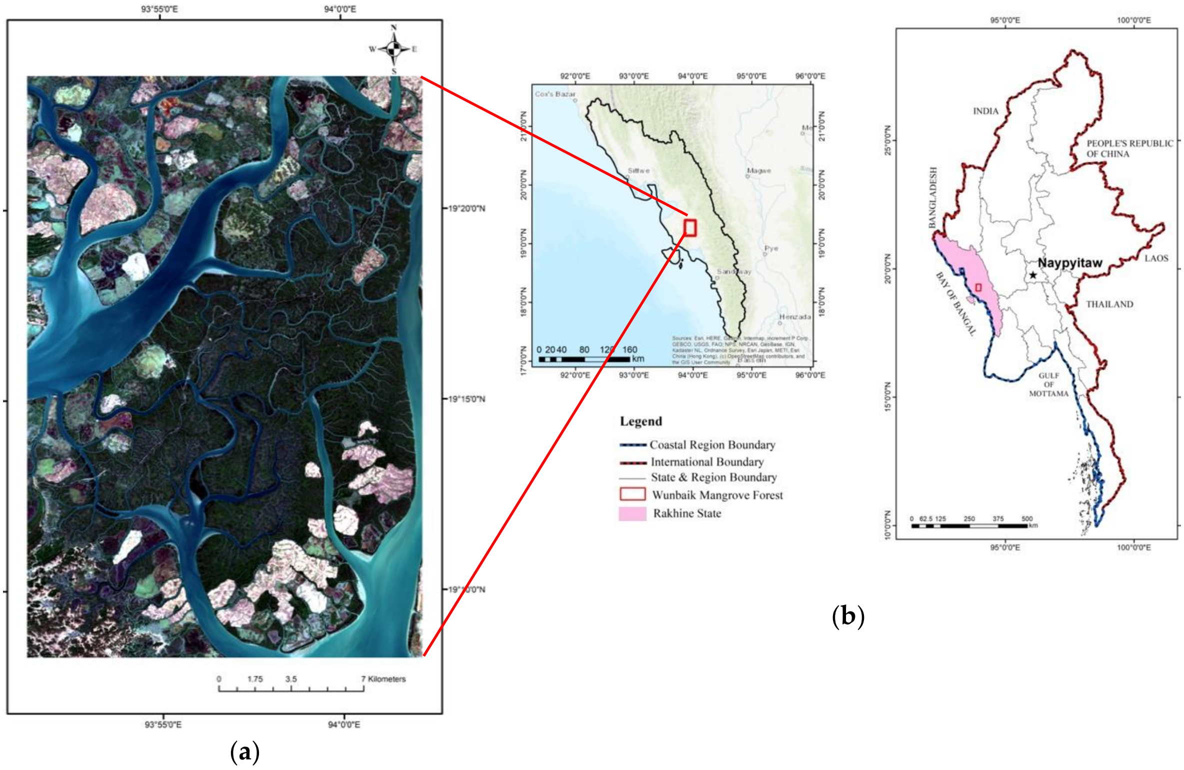

Figure 1. Location of the study area, (a) Wunbaik Mangrove Forest (Sentinel-2 true color image), (b) Rakhine coastal region in Myanmar

3.2.Field Survey

3.2.1 **Discussion with relevant officials and local community**

In order to acquire updated information about the study area, field survey was conducted from September 1, 2019 to October 15, 2019. During the field survey, township staff of FD were interviewed first to know the current status of WMF and mangrove restoration programs. Focus group interview was conducted with the local community of two local villages, Myo Chun and Yan Thit Gyi, in order to understand local livelihood culture and their perspective on mangrove forest.

3.2.2 Collection of ground truthed data for creation of ground truthed image

Being a large extent and various types of land use in the study area, latitudes and longitudes of 80 ground truthed points of different land-use types were collected using a handheld GPS (GARMIN etrex 10), which is able to obtain coordinates with a horizontal accuracy of approximately 3m. These ground truthed points were used to create a ground truthed image in ANN classification.

Preparing accurate ground truthed data is necessary in supervised classification and also a major challenge for training and evaluating a neural network model. In order to obtain a reliable ground truthed image, location points collected in the field were imported to ArcGIS. Using high resolution Google Earth imagery and different combinations of Sentinel-2 satellite bands, polygons were drawn manually by referring to same land cover of the ground truth points. With the aim of accurate mangrove recovery analysis, two major classes were then assigned as mangrove and non-mangrove, rather than multi classification which may lead to massive time consuming for creating ground truth image. Assigned polygons were converted into a raster image with the 10m resolution. A ground truth image, which has assigned values of 0 and 255 for every pixel was obtained. All pixels of 53939393 of which the ground truthed image have width and height of 1914 × 2814 pixel with 10m resolution were counted as the dataset for the ANN prediction.

3.3. Earth Observation Data

To create the required datasets for ANN classification, the sets of multi-spectral bands of Sentinel-2 satellite imagery were collected from the Copernicus Open Access Hub using the semi-automatic classification plugin (SCP) in QGIS [23]. To detect changes to the mangrove and identify recovering mangrove areas within the selected abandoned sites, two dates of cloud-free Sentinel-2 images were utilized; January 21, 2020 and December 23, 2015, which were during the dry seasons. Detailed information about Setinel-2 data acquisition was described in Table 1.

Table 1. Specification of Sentinel-2 product used in this study

Date of Acquisition	Tile Number	Cloud Coverage	Processing Level	Bands Used	Central Wavelength (nm)	Spatial Resolution (m)
January 21, 2020	T46QEG	0	Level-2 A	Band 2	490	10
				Band 3	560	10
				Band 4	665	10
				Band 5	705	20
				Band 6	740	20
December 23, 2015	T46QEG	0	Level-1 C	Band 7	783	20
				Band 8	842	10
				Band 8A	865	20
				Band 11	1910	20
				Band 12	2190	20

The normalized difference vegetation index (NDVI), normalized difference water index (NDWI), and combined mangrove recognition index (CMRI) were used as input features to train the neural network model. NDVI was calculated using band 4 (RED) and band 8 (near infrared (NIR)) [40], while NDWI was derived from using band 3 (GREEN) and band 8 (NIR) [25]. CMRI was determined based on the difference between NDVI and NDWI [26].

We applied SRTM for DSM and MERIT DEM for DTM. During the SRTM mission in February 2000, the SRTM 1 Arc Second DEM was created from the C-band radar data acquired by the cooperation of the National Aeronautics and Space Administration (NASA) and the National Geospatial-Intelligence Agency (NGA). The SRTM1 DEM provides user elevation values with 30 m resolution, referring to the WGS84 ellipsoid as a horizontal datum and geoid as a vertical datum. It may be freely downloaded on the USGS Earthexplorer website (https://earthexplorer.usgs.gov/) [27]. MERIT DEM was downloaded free of charge from the MERIT_DEM website (http://hydro.iis.u-tokyo.ac.jp/~yamadai /MERIT_ DEM/). Moreover, this study used canopy height information to large-scale classification of mangrove extent. Applying the SRTM DEM as a DSM data source is reasonably acceptable in estimating forest height [44], whilst the MERIT DEM provides true topographic information.

3.4. Artificial Neural Network

Considering the structure of the biological neural network of human nervous system, an ANN model primarily consists of multi-layer perceptron (MLP), which has an input layer, hidden layer and output layer, and interconnected operating nodes similar to brain nerve cells in each layer[29]. A basic ANN model was first created by using only one hidden layer with 12 neurons as a basic model in this study. We then explored input parameter and hyperparameter tunings in which different experiments were conducted to obtain the most suitable combination of input features for mangrove classification and an optimum design of an ANN model by tuning number of hidden layers and neurons.

3.5.Workflow of Assessment of Natural Recovery of Mangrove

Figure 2 illustrates the workflow of this research, in which there were three main approaches: (1) input feature selection and hyper-parameter tuning for ANN classification; (2) application of a trained model to a new dataset and improvement of model performance through the transfer learning method; and (3) post-classification change detection. To delineate information on naturally recovering mangroves, the three abandoned sites were extracted from the mangrove change detection results.

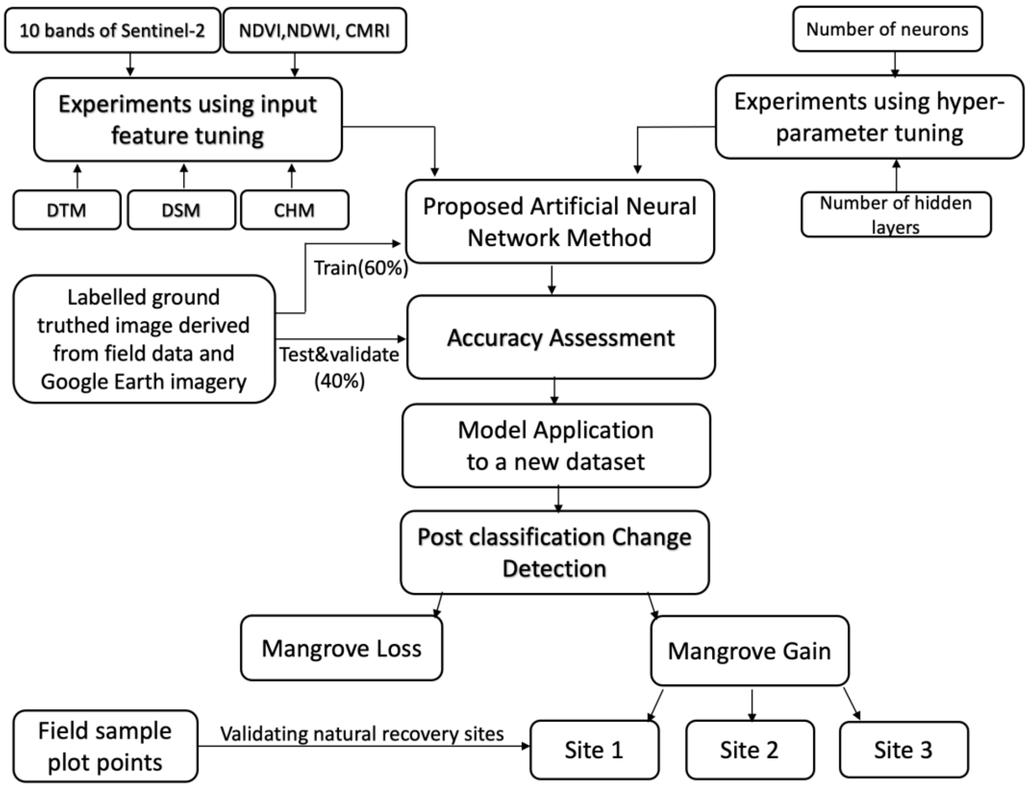

Figure 2. Workflow of assessment of natural recovering mangrove at different abandoned sites

3.6. Accuracy Assessment

Accuracy assessment is one of the major phases in image classification to evaluate model performance. In this study, 20% of the ground truthed information derived from field data was used for cross-validation after training the model. Model performance was evaluated using the overall accuracy and kappa coefficient, the most widely used measures to assess the accuracy of satellite image classification [30]. For the new prediction in 2015 using the ANN model trained with the 2020 dataset, 1000 reference points with geographic locations and ground truthed information, were randomly generated to represent the entire study area. The predicted points were then extracted from the classified images of 2015 and model performance was assessed by comparing them with the reference points.

A confusion or error matrix representing the ground truthed pixels in the column and classified pixels in the row for each class was created to assess the classification accuracy. The overall accuracy was then calculated by dividing the sum of truly classified pixels of each class by the total number of pixels in the diagonal elements of the confusion matrix. The kappa coefficient was also used as it considers the true positive pixels, the false negative pixels, and the non-diagonal elements in a confusion matrix [31], [32]. The kappa coefficient ranges from 0 to 1; the closer it is to 1, the higher the classification accuracy.

4. Results and Discussions

4.1 Experimental Results for Input Features Selection

Of total 15 experiments after conducting different classifications by adjusting input features, the experiment 6, which contains 10 bands of Sentinel-2 image, NDVI, NDWI, MERIT DEM and CHM yielded not only highest accuracy but also smooth pixel structure of the output image for mangrove distribution. The resultant overall accuracies of all experiments were described in Table 2.

Table 2. Experimental results of input feature adjustment

Experiment	Combination of input features	Overall accuracy
1	10 bands (B2, B3, B4, B5, B6, B7, B8, B8A, B11, B12) of Sentinel-2 image	56.39%
2	10 bands, NDVI, NDWI	93.43%
3	10 bands, NDVI, NDWI, CMRI	94.02%
4	10 bands, NDVI, NDWI, MERIT	95.49%
5	10 bands, MERIT	71.05%
6	10 bands, NDVI, NDWI, MERIT, CHM	95.85%
7	10 bands, NDVI, NDWI, MERIT, SRTM	95.79%
8	10 bands, NDVI, NDWI, SRTM, CHM	93.71%
9	10 bands, NDVI, NDWI, MERIT, SRTM, CHM	93.73%
10	10 bands, NDVI, NDWI, CHM	95.33%

11	10 bands, MERIT, CMRI	72.00%
12	10 bands, NDVI, NDWI, CMRI, MERIT	95.70%
13	10 bands, NDVI, NDWI, CMRI, MERIT, CHM	95.81%
14	NDVI, NDWI, MERIT, CHM	95.76%
15	4 selected bands (B2, B3, B4, B8), NDVI, NDWI, MERIT, CHM	95.65%

3.1.2. Experimental Results of Hyper-Parameter Tuning

Using the dataset in Experiment 6 from the input parameter tuning section, hyper-parameter tuning was evaluated by adjusting the number of hidden layers and neurons. First, one hidden layer with 10 neurons was added to the basic model used in the input feature adjustment. The model trained and evaluated the accuracy, while visually checking the behavior of the model in the learning curves of accuracy and loss using the validation dataset. Following the addition of up to four hidden layers, the model with two hidden layers (12:10), produced the highest accuracy of 95.89%. The accuracy of the model with three hidden layers (12:10:8) and four hidden layers (12:10:10:8) was the same at 95.76%.

The neurons in the hidden layers play a key role as processing units in analyzing input data and producing output; hence, the number of neurons influences the performance of an ANN model. The number of neurons in the two selected hidden layers was adjusted by halving and doubling the neurons in each layer for testing the performance. Comparing the accuracy and loss of training prediction to that of validation in each model, the model with greater neurons (544:320) performed with the highest accuracy of 95.98%, least error, and had the smallest difference between training and validation predictions. After conducting input feature and hyper-parameter tuning, the ANN model with two hidden layers (544:320 neurons) was selected as the model for mangrove classification using the input features of Experiment 6 (Figure 3).

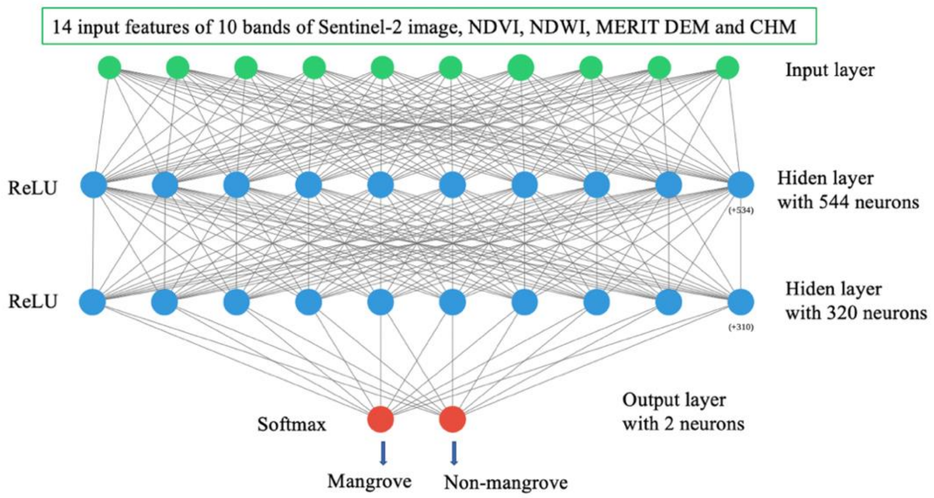

Figure 3. Proposed ANN model and input dataset for classification of mangrove distribution

3.2. Classification Results of New Prediction using Transfer Learning

The ANN model with two hidden layers (544:320), obtained through hyper-parameter tuning, was applied to a new dataset from 2015, with the same input features. The model produced an overall accuracy of 94.50% and a kappa coefficient of 0.92. Despite the high classification accuracy, the model classified green paddy fields as mangroves falsely in the new prediction due to the spectral variation in different seasons. To overcome this problem, some parameters of the original model were fixed with existing knowledge while others were retrained with a new dataset that contained information on the green paddy fields (Figure 4).

The classification results of the experiments are described in

Table 3. The original model produced a low accuracy of 72.59% for the transfer learning dataset due to the spectral variation problem in paddy fields. The original model was tested with different settings of layer fixing and re-training. Of the six different models re-trained in transfer learning, the T12 model, which fixed the second hidden layer (layer 1) and output layer (layer 2), could be trained within the shortest training time of 32 s per epoch (using one node on the supercomputer ITO-B at Kyushu University). The T12 model also outperformed other models, obtaining the highest accuracy of 97.2% and a kappa coefficient of 0.94 for the whole dataset and a high accuracy of 95.77% for the transfer learning dataset. As a result, the T12 model could eliminate misclassified paddy field pixels predicted by the original model. After conducting mangrove classifications using the ANN model in 2020 and 2015, final mangrove distribution maps of the two periods are shown in Figure 5(a and b), respectively.

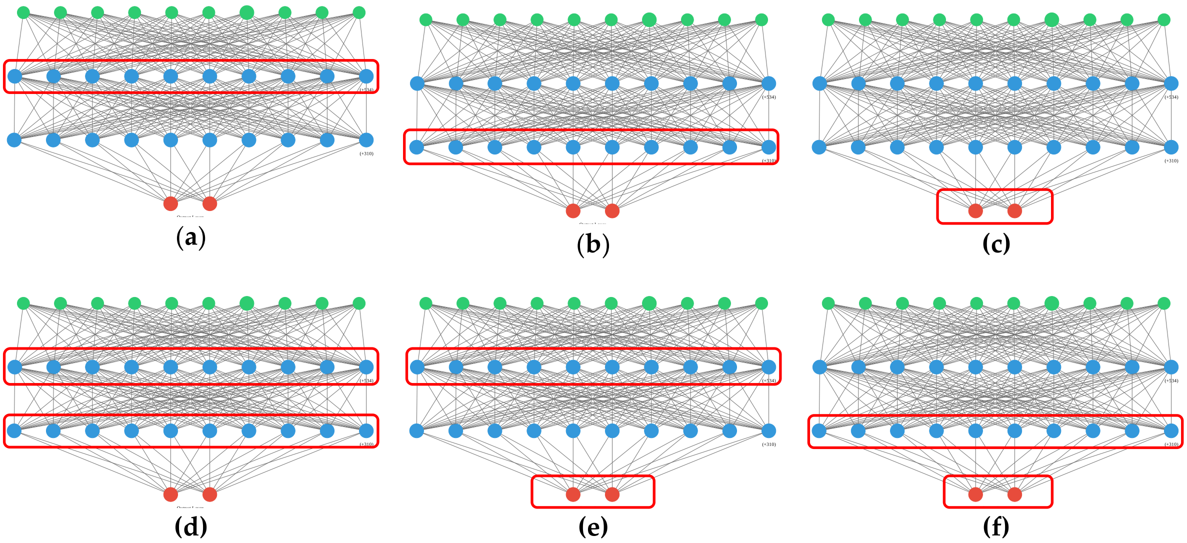

Figure 4. Six different types of models in transfer learning process: (a) T0 model fixed layer 0, (b) T1 model fixed layer 1, (c) T2 model fixed layer 2, (d) T01 model fixed layer 0 and 1, (e) T02 model fixed layer 0 and 2, and (f) T12 model fixed layer 1 and 2

Table 3. Classification results of different models in transfer learning

Models	**Transfer learning dataset**		**Accuracy for whole dataset (%)**
	Accuracy (%)	Training time per epoch	
Original model	72.59	-	94.5
T0 (Model fixed layer 0)	96.09	42s	93.8
T1 (Model fixed layer 1)	95.83	33s	95.10
T2 (Model fixed layer 2)	96.07	40s	93.00
T01 (Model fixed layer 0 and 1)	95.57	38s	94.00
T02 (Model fixed layer 0 and 2)	96.04	38s	96.20
T12 (Model fixed layer 1 and 2)	95.77	32s	97.20

3.3. Mangrove Changes and Drivers

To provide updated information on the mangrove distribution in WMF, we examined spatial changes of mangroves between 2015 and 2020. By differentiating between classified images in 2015 and 2020, the change detection result showed significant changes in the mangrove extent in the WMF (Figure 5(c)). To focus on the major causes of mangrove loss and gain, only extensive change areas were examined and validated with Sentinel-2 true color imagery (10 m resolution) and very high resolution (1 m) Google Earth imagery.

Interpreting change detection results based on field information and mangrove losses in the study area between 2015 and 2020, is warranted due to the expansion of shrimp ponds, while mangrove gain patches were detected at plantation sites, and naturally regenerated areas. The locations of artificial mangrove plantations established by the Forest Department could be identified using high-resolution Google Earth imagery and GPS points collected during the field survey. Naturally recovered mangroves were found in active shrimp ponds, abandoned sites, and tidal flats. Between 2015 and 2020, the total mangrove area declined from 254.30 km^2 to 249.83 km^2 slightly, while the non-mangrove area increased from 284.30 km^2 to 288.77 km^2.

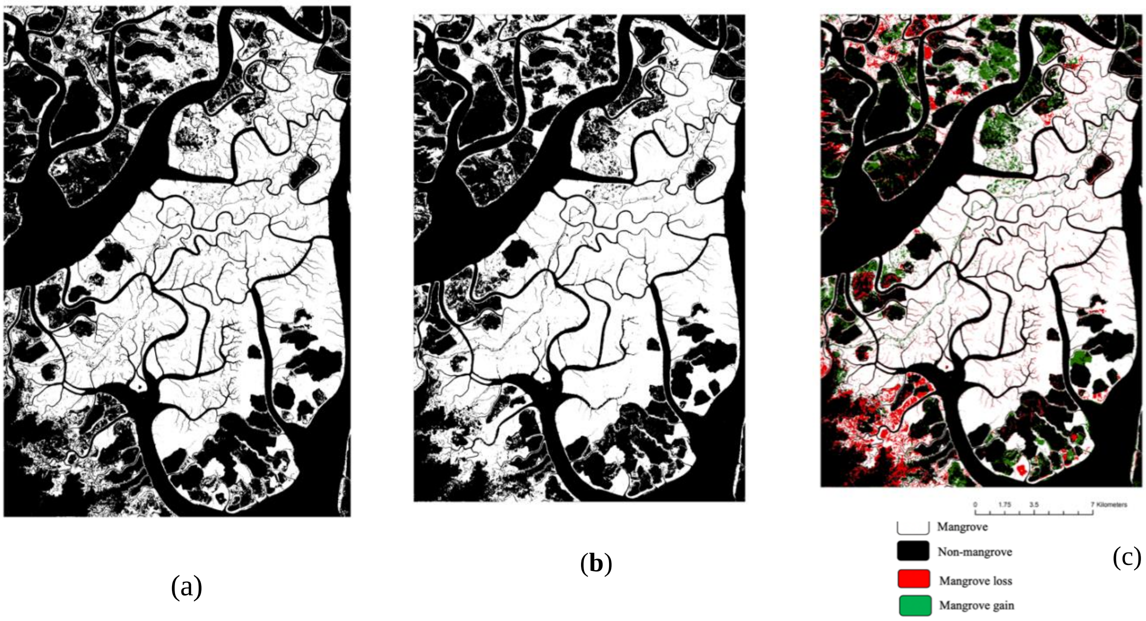

Figure 5. Mangrove distribution maps of Wunbaik Mangrove Forest in (a) 2020, (b) 2015 predicted by the proposed ANN method, and (c) mangrove forest changes between 2015 and 2020

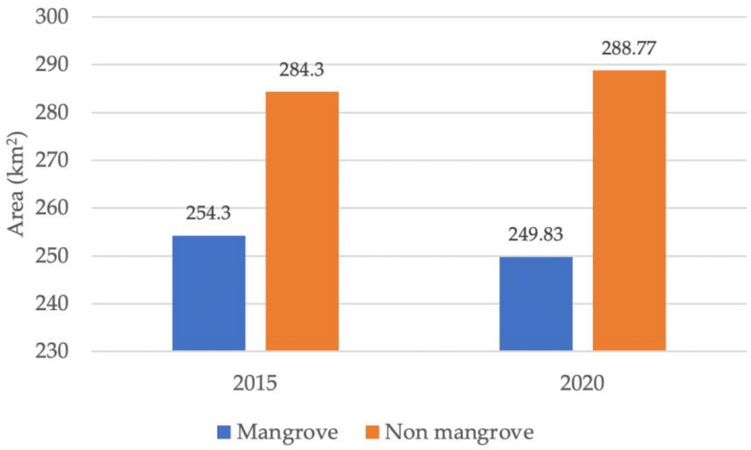

Figure 6. Land cover dynamic in WMF between 2015 and 2020

3.3. Natural Recovery of Mangroves at Abandoned Sites

To delineate the naturally recovering mangroves in the study area, three abandoned shrimp ponds selected during the field survey were extracted from the results of change detection. The recovering mangrove area in each abandoned pond was then evaluated and compared to the extent of the abandoned sites in ArcGIS. During the abandonment period from 2015 to 2020, mangrove cover increased by 49.02% at Site 1, 55.93% at Site 2, and 50.00% at Site 3 (**Error! Reference source not found.**). The results showed that mangroves can naturally ecover in approximately half of the abandoned sites without any artificial effort (**Error! Reference source not found.**).

Based on the field survey and collaboration with Forest Department staff and shrimp pond owners, it was confirmed that there was no artificial planting following the abandonment of these shrimp ponds. The recovering mangrove areas were validated using ground truth GPS points of 50 sample plots collected in the three recovery sites and 12 different mangrove species were identified through the field inventory. *Avicennia officinalis* (Figure 7(a)) was the dominant species at Site 1, while *A. marina* (Figure 7(b,c)) dominated the other species at sites 2 and 3.

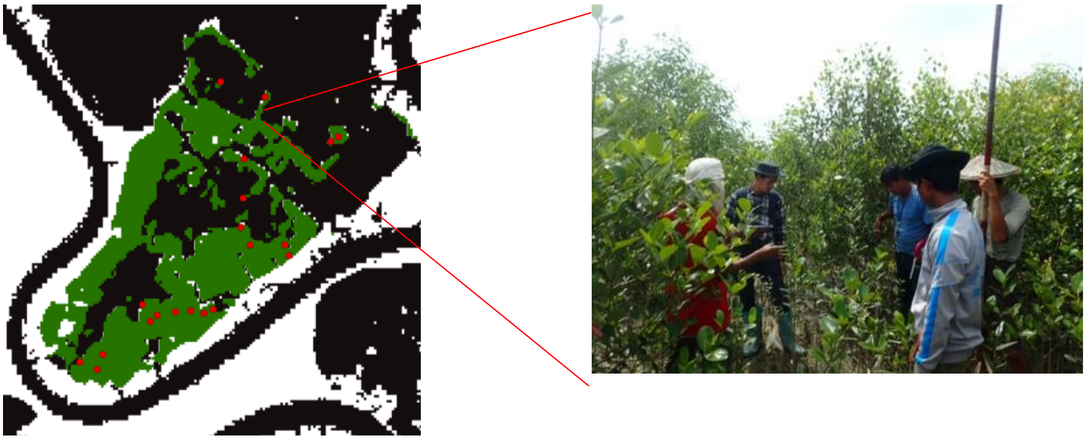

(a)

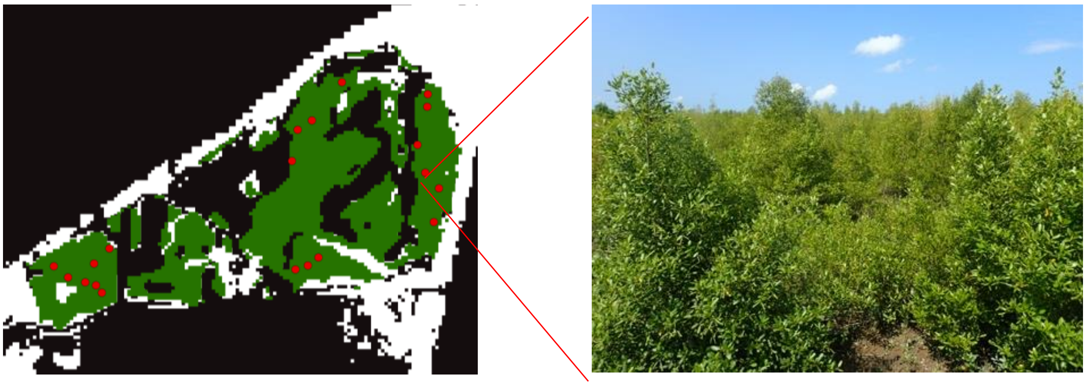

(b)

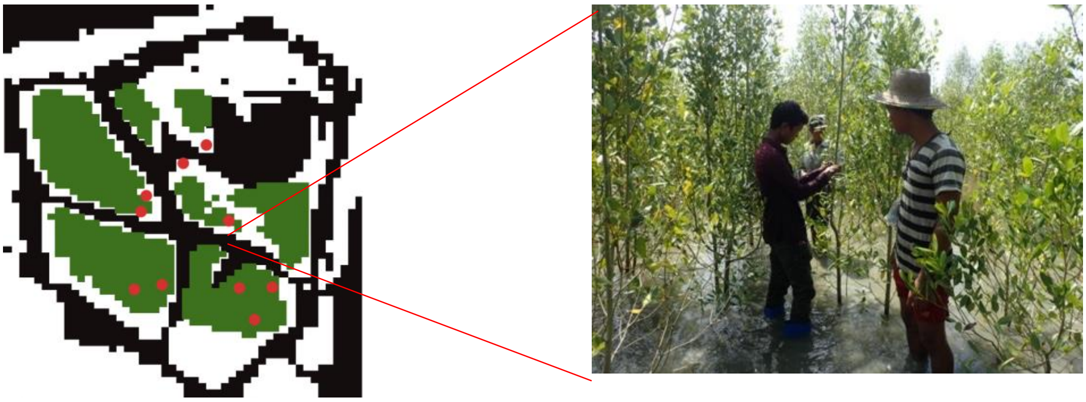

(c)

Figure 7. Ground checked photos of naturally recovering mangrove species at (a) site 1 dominating *Avicennia officinalis*, (b) site 2, and (c) site 3 dominating *Avicennia marina*

3.4. Species Composition and Diversity

For all 50 sample plots of the three recovering sites, 12 different mangrove species could be identified through field inventory. Of these mangrove species recorded at three recovered sites, 11 mangrove species were found at site 1 while 8 and 3 species at site 2 and 3 respectively. Through IVI analysis, *Avicennia officinalis* was the most dominant species with highest IVI values at site 1(Table 4). On the other hand, *Avicennia marina* which possesses higher IVI values than other species predominated at site 2 and 3 (Table 5 and Table 6).

Shannon indices expressed in Figure 8 inform that three recovering sites have different diversity of mangrove species. Shannon diversity index (H), evenness (E) and richness (Hmax) for site 1 were 1.19, 0.5 and 2.4 whereas 0.76, 0.37 and 2.08 for site 2 and 0.3, 0.28 and 1.1 for site 3, respectively.

Table 4. IVI values of recovered mangrove species at site 1

Species	Relative Frequency	Relative density	Relative dominance	IVI
Avicennia officinalis	28.5714	69.4444	39.1836	137.1995
Sonneratia apetala	22.8571	10.4167	31.3693	64.6431
Sonneratia alba	17.1429	7.2917	10.9234	35.3580
Avicennia alba	11.4286	3.8194	11.9427	27.1907
Avicennia marina	7.1429	2.4306	3.7594	13.3328
Bruguiria gyumnoriza	4.2857	1.3889	1.0044	6.6791
Rizophora apiculata	2.8571	0.6944	1.1826	4.7342
Ceriops decendra	1.4286	1.0417	0.1496	2.6198
Aegiceras corniculatum	1.4286	1.3889	0.2095	3.0269
Heritiera Fomes	1.4286	1.3889	0.1932	3.0107
Xylocarpus granatum	1.4286	0.6944	0.0822	2.2052

Table 5. IVI values of recovered mangrove species at site 2

Species	**Relative Frequency**	**Relative density**	**Relative dominance**	**IVI**
Avicennia marina	38.4615	82.3961	89.5546	210.4122
Rizophora apiculata	21.1538	4.1565	4.7681	30.0785
Aegialistis rotundifolia	9.6154	4.6455	0.7159	14.9768
Ceriops decendra	7.6923	4.1565	0.7423	12.5911
Bruguiria gyumnoriza	7.6923	1.2225	0.3248	9.2396
Avicennia officinalis	9.6154	2.4450	2.0858	14.1461
Sonneratia apetala	1.9231	0.4890	0.6542	3.0663
Avicennia alba	3.8462	0.4890	1.1543	5.4895

Table 6. IVI values of recovered mangrove species at site 3

Species	Relative Frequency	Relative density	Relative dominance	IVI
Avicennia marina	52.6316	92.7835	94.5877	240.0028
Avicennia officinalis	31.5789	5.1546	4.6917	41.4253
Aegialistis rotundifolia	15.7895	2.0619	0.7205	18.5719

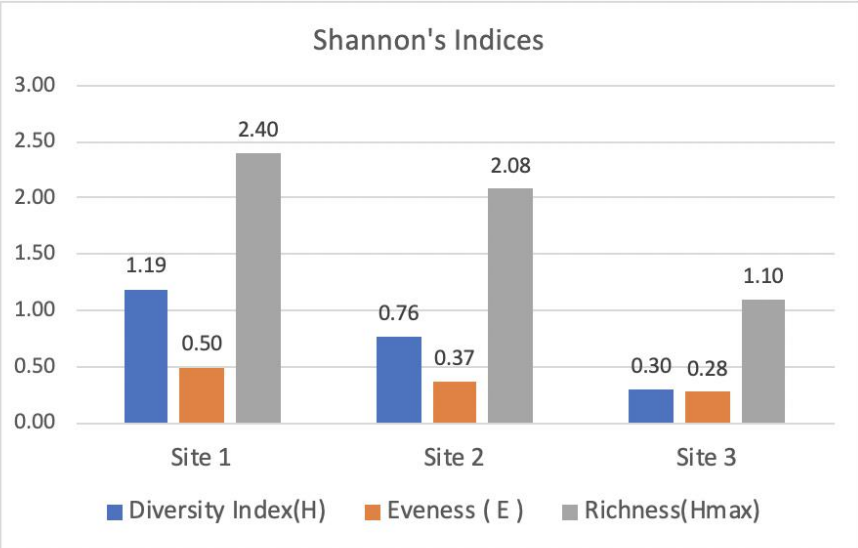

Figure 8. Shannon's indices of three different recovering sites

3.4.1 Environmental Preference of Recovered Mangrove Species

Without considering the environmental preference of mangrove species, it would be difficult to achieve successful mangrove plantations if there were needed to plant artificially at where mangrove species have no chance for natural recovery. Different mangrove species have different salinity preferences that would be indicator species with respect to salinity [33]. The recovering mangrove species were observed with their preference of salinity and elevation range in this study. *A.officinalis* and *A.marina* could be found at both low and high salinity range while *Aegialistis rotundifolia* is only at high salinity range (Figure 9). This finding is consistent with the results of experimental analyses in other studies [34], [35] in which different mangrove species were tested with different salinity levels. Their experimental results also reveal that due to having salt-secreting glands in the leaves of *A. marina*, this species is more salt tolerant than other species. Moreover, San Win et al[36] found *Avicennia* species at both low and high salinity ranges (0.5-28.9 PSU) of the Ayeyarwaddy mangrove region, Myanmar. As *A. officinalis* and *A. marina* were recorded at 31 and 35 out of the total 50 sample plots in this study, these species have a high adaptivity to any environmental conditions at abandoned sites.

In case of elevation range, *Bruguiria gyumnoriza* and *Ceriops decendra* were occurred at only high range within the sample plots (Figure 10). There is however no significant difference of elevation among recovered species in the study area because the mangrove area is a flattened surface of the inland region.

It is not straightforward to approve the determinant of distribution of mangrove species because there are many physical factors such as tidal inundation, source of seed-productive trees, and seed sizes which should be considered for seed dispersal. This study therefore showed the occurrence of salinity and elevation ranges in which each species was recorded at recovering sites during field survey. The information about environmental preferences of recovered species related with the abandoned sites should be well noted for practitioners in implementing restoration projects. By referring to this information, suitable mangrove species can be selected depending on the salinity and elevation of the restoration sites.

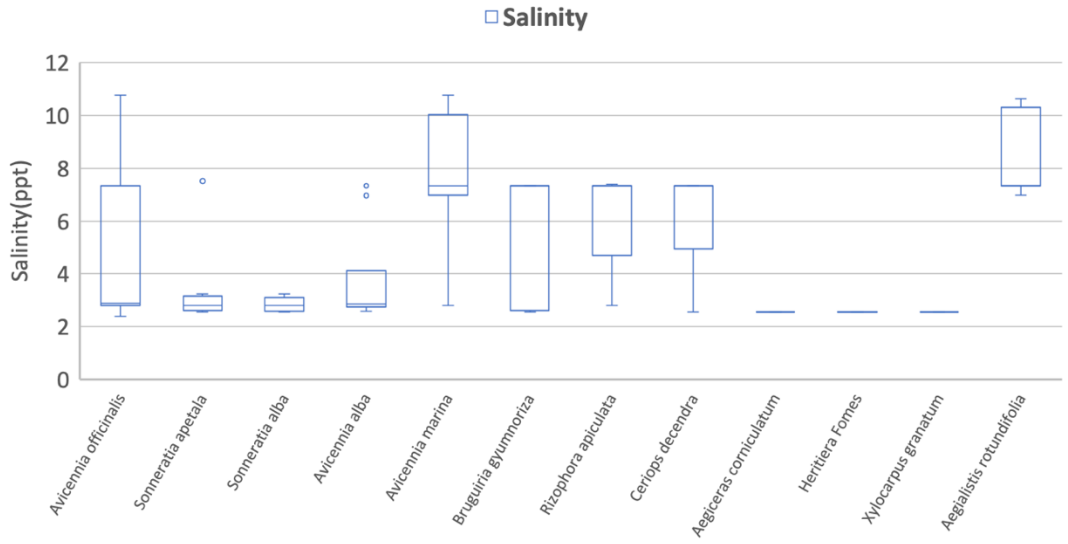

Figure 9. Salinity range of different recovered mangrove species

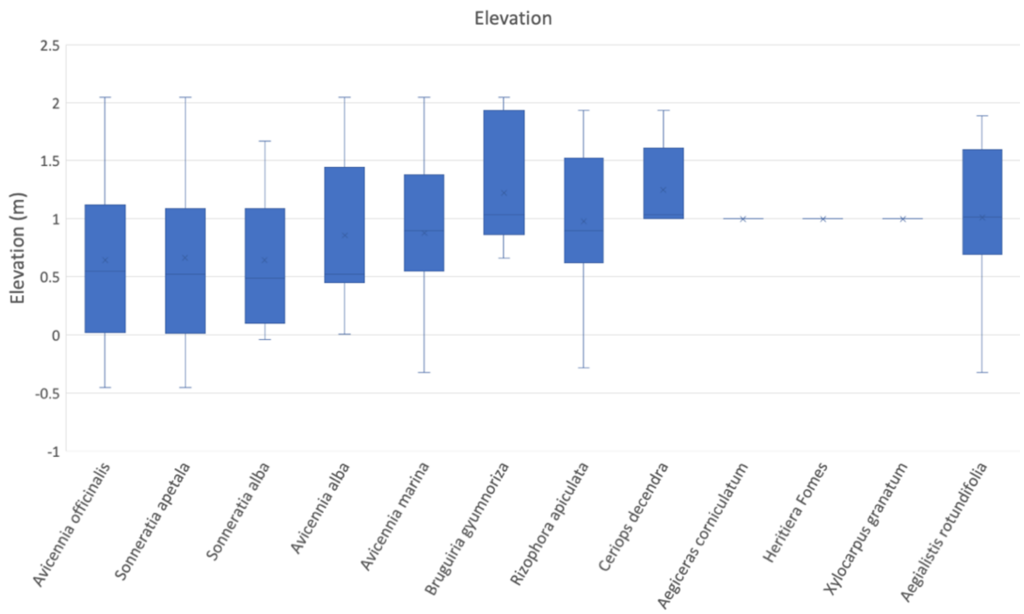

Figure 10. Elevation range of different recovered mangrove species

5. Conclusions

This study was the first attempt employing ANN classification using Sentinel-2 imagery for mangrove classification. We explored two main experiments relating to input feature and hyper-parameter tuning. Through these experiments, we proposed a promising ANN model applying Sentinel-2 satellite imagery, and topographic and canopy height information for constraining mangrove distribution. Through optimization, we achieved the highest overall accuracy of 95.98% and a kappa coefficient of 0.92. Moreover, we used the transfer learning approach to improve the ANN model performance and produced a high overall accuracy of 97.20% and a kappa coefficient of 0.94. The model created can be deployed for mangrove classification in different seasons and regions.

The outcomes of this study also contribute to the production of up-to-date and reliable information regarding mangrove change in the WMF through post-classification change detection. The results highlight that mangrove extent has decreased in the WMF between 2015 and 2020 owing to the expansion of shrimp ponds. By integrating field observations with the change detection results, we highlight that the mangroves were able to naturally recover in approximately 50% of the abandoned sites within a short abandonment period. Further research attention should be given to the natural recovery process of mangroves, as it presents a valuable opportunity for mangrove rehabilitation following human disturbance.

Acknowledgments:

The ANN computation was carried out using the computer resource offered under the category of General Projects by Research Institute for Information Technology, Kyushu University. I am also thankful to Dr. Dai Yamzaki, Associate Professor, Institute of Industrial Science, The University of Tokyo for providing MERIT DEM. The author is deeply indebted to Asian Development Bank for financial support during the study period in Japan.

Reference:

[1] A. Mitra, *Sensitivity of mangrove ecosystem to changing climate*. 2013.
[2] M. Spalding, *World Atlas of Mangroves*. 2010.
[3] D. M. Alongi, “Present state and future of the world’s mangrove forests,” *Environ. Conserv.*, vol. 29, no. 3, pp. 331–349, 2002.
[4] D. O. Stanley, J. Broadhead, M. Aung Aung, Burma. Forest Department., and Food and Agriculture Organization of the United Nations., “The atlas and guidelines for mangrove management in Wunbaik Reserved Forest,” *FAO-UN, Myanmar Publ.*, no. 2011/04, pp. iii, 132 p., 2011.
[5] C. Giri, “Observation and monitoring of mangrove forests using remote sensing: Opportunities and challenges,” *Remote Sens.*, vol. 8, no. 9, p. 783, 2016.
[6] D. Lu and Q. Weng, “A survey of image classification methods and techniques for improving classification performance,” *Int. J. Remote Sens.*, vol. 28, no. 5, pp. 823–870, 2007.
[7] M. S. M. Altaei, “Satellite Image Classification Using Artificial Neural Network,” *Int. J. Res. Advent Technol.*, vol. 7, no. 1, pp. 459–462, 2019.
[8] M. Toshniwal, “Satellite image classification using neural networks,” *3rd Int. JConference Sci. Electron. Technol. Inf. Telecommun.*, pp. 1–5, 2005.
[9] G. Ge, Z. Shi, Y. Zhu, X. Yang, and Y. Hao, “Land use/cover classification in an arid desert-oasis mosaic landscape of China using remote sensed imagery: Performance assessment of four machine learning algorithms,” *Glob. Ecol. Conserv.*, vol. 22, p. e00971, 2020.
[10] D. Kawabata and J. Bandibas, “Landslide susceptibility mapping using geological data, a DEM from ASTER images and an Artificial Neural Network (ANN),” *Geomorphology*, vol. 113, no. 1–2, pp. 97–109, 2009.
[11] European Space Agency, “ESA - About the launch.” [Online]. Available: https://www.esa.int/Applications/Observing_the_Earth/Copernicus/Sentinel-2/About_the_launch. [Accessed: 30-Jun-2020].
[12] H. Astola, T. Häme, L. Sirro, M. Molinier, and J. Kilpi, “Comparison of Sentinel-2 and Landsat 8 imagery for forest variable prediction in boreal region,” *Remote Sens. Environ.*, vol. 223, no. October 2017, pp. 257–273, 2019.
[13] P. García-Llamas *et al.*, “Evaluation and comparison of Landsat 8, Sentinel-2 and Deimos-1 remote sensing indices for assessing burn severity in Mediterranean fire-prone ecosystems,” *Int. J. Appl. Earth Obs. Geoinf.*, vol. 80, no. February, pp. 137–144, 2019.
[14] T. A. Lima, R. Beuchle, A. Langner, R. C. Grecchi, V. C. Griess, and F. Achard, “Comparing Sentinel-2 MSI and Landsat 8 OLI Imagery for Monitoring Selective Logging in the Brazilian Amazon,” *Remote Sens.*, vol. 11, no. 8, p. 961, 2019.
[15] G. Connette, P. Oswald, M. Songer, and P. Leimgruber, “Mapping distinct forest types improves overall forest identification based on multi-spectral landsat imagery for Myanmar’S Tanintharyi Region,” *Remote Sens.*, vol. 8, no. 11, p. 882, 2016.
[16] R. S. Morgan, M. A. El-Hady, and I. S. Rahim, “Soil salinity mapping utilizing sentinel-2 and neural networks,” *Indian J. Agric. Res.*, vol. 52, no. 5, pp. 524–529, 2018.
[17] J. Mohite, N. Twarakavi, and S. Pappula, “Evaluating the Potential of Sentinel-2 for Low Severity Mites Infestation Detection in Grapes,” *IGARSS 2018 - 2018 IEEE Int. Geosci. Remote Sens. Symp. Val.*, pp. 4651–4654, 2018.
[18] J. E. Pereira-Pires, V. Aubard, R. A. Ribeiro, J. M. Fonseca, J. M. N. Silva, and A. Mora, “Semi-automatic methodology for fire break maintenance operations detection with sentinel-2 imagery and artificial neural network,” *Remote Sens.*, vol. 12, no. 6, p.

909, 2020.
[19] V. Kristollari and V. Karathanassi, “Artificial neural networks for cloud masking of Sentinel-2 ocean images with noise and sunglint,” *Int. J. Remote Sens.*, vol. 41, no. 11, pp. 4102–4135, 2020.
[20] Y. S. Lee, S. Lee, and H. S. Jung, “Mapping forest vertical structure in Gong-Ju, Korea using sentinel-2 satellite images and artificial neural networks,” *Appl. Sci.*, vol. 10, no. 5, p. 1666, 2020.
[21] A. A. Saw and M. Kanzaki, “Local Livelihoods and Encroachment into a Mangrove Forest Reserve: A Case Study of the Wunbaik Reserved Mangrove Forest, Myanmar,” *Procedia Environ. Sci.*, vol. 28, no. Sustain 2014, pp. 483–492, 2015.
[22] M. Win, “The mangrove vegetation of Wubaik Reserved Forest,” *FAO-UN, Myanmar Publ.*, no. 2011/04, pp. iii, 191 p., 2011.
[23] Congedo Luca, *Semi-Automatic Classification Plugin Documentation*. 2016.
[24] P. M. Teillet, K. Staenz, and D. J. Williams, “Effects of spectral, spatial, and radiometric characteristics on remote sensing vegetation indices of forested regions,” *Remote Sens. Environ.*, vol. 61, no. 1, pp. 139–149, 1997.
[25] S. K. McFeeters, “The use of the Normalized Difference Water Index (NDWI) in the delineation of open water features,” *Int. J. Remote Sens.*, vol. 17, no. 7, pp. 1425–1432, 1996.
[26] K. Gupta *et al.*, “An index for discrimination of mangroves from non-mangroves using LANDSAT 8 OLI imagery,” *MethodsX*, vol. 5, no. May, pp. 1129–1139, 2018.
[27] L. Yap, L. H. Kandé, R. Nouayou, J. Kamguia, N. A. Ngouh, and M. B. Makuate, “Vertical accuracy evaluation of freely available latest high-resolution (30 m) global digital elevation models over Cameroon (Central Africa) with GPS/leveling ground control points.,” *Int. J. Digit. Earth*, vol. 12, no. 5, pp. 500–524, 2019.
[28] W. J. Lee and C. W. Lee, “Forest canopy height estimation using multiplatform remote sensing dataset,” *J. Sensors*, vol. 2018, pp. 1–9, 2018.
[29] C. C. Aggarwal, *Neural Networks and Deep Learning*. 2018.
[30] S. S. Rwanga and J. M. Ndambuki, “Accuracy Assessment of Land Use/Land Cover Classification Using Remote Sensing and GIS,” *Int. J. Geosci.*, vol. 08, no. 04, pp. 611–622, 2017.
[31] R. G. Congalton, “Assessing Landsat Classification Accuracy Using Discrete Multivariate Analysis Statistical Techniques,” *Photogramm. Eng. Remote SENSING; Vol. 49; No. 12; December 1983; pp. 1671-1678.*, vol. 27, no. 2, pp. 83–92, 1983.
[32] J. Cohen, “A Coefficient of Aggrement for Normal Scales,” *Curr. Contents*, vol. 20, pp. 37–46, 1960.
[33] J. Barik, A. Mukhopadhyay, T. Ghosh, S. K. Mukhopadhyay, S. M. Chowdhury, and S. Hazra, “Mangrove species distribution and water salinity: an indicator species approach to Sundarban,” *J. Coast. Conserv.*, vol. 22, no. 2, pp. 361–368, 2018.
[34] B. F. Clough, “Growth and salt balance of the mangroves Avicennia marina (Forsk.) Vierh. and Rhizophora stylosa Griff. in relation to salinity.,” *Aust. J. Plant Physiol.*, vol. 11, no. 5, pp. 419–430, 1984.
[35] M. A. Khan and I. Aziz, “Salinity tolerance in some mangrove species from Pakistan,” *Wetl. Ecol. Manag.*, vol. 9, no. 3, pp. 219–223, 2001.
[36] S. Win, S. Towprayoon, and A. Chidthaisong, “Adaptation of mangrove trees to different salinity areas in the Ayeyarwaddy Delta Coastal Zone, Myanmar,” *Estuar. Coast. Shelf Sci.*, vol. 228, no. July, 2019.